

# N-order bright and dark rogue waves in a resonant erbium-doped fibre system

Jingsong He<sup>a</sup>, Shuwei Xu<sup>b</sup>, and K. Porseizan<sup>c</sup>

<sup>a</sup>Department of Mathematics, Ningbo University, Ningbo, Zhejiang 315211, P.R. China.

<sup>b</sup>School of Mathematical Sciences, USTC, Hefei, Anhui 230026, P.R. China.

<sup>c</sup>Department of Physics, Pondicherry University, Puducherry 605014, India.

The rogue waves in a resonant erbium-doped fibre system governed by a coupled system of the nonlinear Schrödinger equation and the Maxwell-Bloch equation (NLS-MB equations) are given explicitly by a Taylor series expansion about the breather solutions of the normalized slowly varying amplitude of the complex field envelope  $E$ , polarization  $p$  and population inversion  $\eta$ . The n-order breather solutions of the three fields are constructed using Darboux transformation (DT) by assuming periodic seed solutions. What is more, the n-order rogue waves are given by determinant forms with  $n + 3$  free parameters. Furthermore, the possible connection between our rogue waves and the generation of supercontinuum generation is discussed.

PACS numbers: 02.30.Ik, 42.81.Dp, 52.35.Bj, 52.35.Sb, 94.05.Fg

## I. INTRODUCTION

In recent years, long haul optical communication through fibers has attracted considerable interest in research activities among scientists all over the world. Especially, it has been demonstrated that the soliton-type pulse propagation will play a vital role in the ultra fast communication systems. They are considered to be the futuristic tools in achieving low-loss, cost-effective high speed communication throughout the world. Soliton-type pulse propagation through nonlinear optical fibers is realized by means of the exact counterbalance between the major constraints of the fiber, viz., group velocity dispersion (linear effect) which broadens the pulse and the self-phase modulation (nonlinear effect) which contracts the pulse. The propagation of optical pulses through a nonlinear fiber in the picosecond regime is described by the well-known nonlinear Schrödinger (NLS) equation, which was first proposed by Hasegawa and Tappert in 1973[1].

To make the soliton based communication systems highly competitive, reliable and economical when compared to the conventional systems, attenuation in a fiber must be compensated. A different type of optical soliton is associated with the self-induced transparency (SIT) effect in resonant absorbers. The soliton pulse propagation in an erbium doped fiber amplifier utilizes the SIT phenomena, first discovered by McCall and Hahn[2]. In 1967, McCall and Hahn proposed a new type of optical soliton in a two level resonant system. Above a well-defined threshold intensity, short resonant pulses of a given duration will propagate through a normally absorbing medium with anomalously low attenuation. This happens when the pulse width is short, compared to the relaxation times in the medium and the pulse centre frequency is in resonance with a two-level absorbing transition. After a few classical absorption lengths, the pulse achieves a steady state in which its width, energy and shape remain constant. The pulse velocity has greatly reduced from the normal velocity of light in such media. With these properties, the pulse propagation of this type

is named "self-induced transparency" (SIT) soliton and frequently described by the Maxwell-Bloch (MB) equations. They are

$$\begin{aligned} E_z &= p, \\ p_t &= i \omega_0 p - f q \eta, \\ \eta_t &= f (q p^* + q^* p), \end{aligned} \quad (1)$$

Here,  $E$  and  $p$  are complex variables,  $\eta$  is a real variable and  $\omega_0$  is a real constant and  $f$  is the character describing the interaction between the resonant atoms and the optical field. The symbol  $*$  denotes the complex conjugate. These equations can be extended to the case of fiber amplifiers. When Er is doped with the core of the optical fibres, then the nonlinear wave propagation can have both the effects due to silica and Er impurities. Er impurities give SIT effect to the optical pulse, whereas the silica material gives the NLS soliton effect. So if we consider these effects for a large width pulse, then the system dynamics will be governed by the coupled system of the NLS equation and the MB equation (NLS-MB system). Considering the Erbium doped in nonlinear silica waveguides, for the first time, the combined NLS-MB system was proposed by Maimistov and Manykin [3, 4] in 1983. They have also constructed the Lax pair and used the inverse scattering transform technique for the generation of soliton solution. The NLS-MB equations read as[3-5]

$$\begin{aligned} E_t &= i \left[ \frac{1}{2} E_{xx} + |E|^2 E \right] + 2p, \\ p_x &= 2i \omega_0 p + 2E \eta, \\ \eta_x &= - (E p^* + E^* p), \end{aligned} \quad (2)$$

The above equation have also been reduced through the Painleve analysis [6]. Further, Kakei and Satsuma [7] also reported the Lax pair and the multi-soliton solution of the NLS-MB equations. The integrability aspects of NLS-MB system with variable dispersion, the study of propagation of optical solitons in coupled NLS-MB,

and random nonuniform-doped media have been reported earlier wherein the spectral parameter was kept constant. The coexistence of NLS soliton and SIT soliton has already been confirmed experimentally [10, 11]. The propagation and switching of SIT in nonlinear directional couplers with two-level atom nonlinearity has been recently investigated numerically by retaining the transverse dependence of the optical field and atomic variable. Recent experiments by Nakazawa *et al.*, have confirmed guided wave SIT soliton formation and propagation by employing a few meters of erbium doped fibre [8–11].

Recently, considering all higher order effects in the propagation of femtosecond pulses, the coupled Hirota and Maxwell-Bloch (CH-MB) equations have been proposed and analyzed for soliton solutions [12]. Some generalization of NLS-MB equations, for instance, the CH-MB equations and the NLS-MB equations with variable dispersion and nonlinear effects are discussed [13–15]. The single soliton and the single breather solutions [16] of the NLS-MB equations are given by the Darboux transformation (DT) [17, 18]. Soliton solution for the generalized coupled variable coefficient NLS-MB system was also investigated by the DT [19] and the Hirota method [20].

In recent years, in addition to solitons in different optical systems, the study of rogue waves have also attracted considerable interest because of their potential applications in different branches of physics including oceanography [21–24], which occurs due to either modulation instability [25–31], or random initial condition [24, 32]. The first order rogue wave is most likely to appear as a single peak hump with two caves in a plane with a nonzero boundary. One of the possible generating mechanisms for rogue waves is the creation of breathers which can be realized by modulation instability. Then, larger rogue waves can build up when two or more breathers collide themselves [33–39]. Recently, more general higher-order rogue waves were obtained such as showing that these general  $N$ -th order rogue waves contain  $(N - 1)$  free irreducible complex parameters [37]. Rogue waves can also be observed in space plasmas [40–45] and optics when propagating high power optical radiation through photonic crystal fibers [46–48]. Considering all higher order effects in the propagation of femtosecond pulses, rogue waves can also be observed in a system modeled by the Hirota equation [49–51]. Furthermore, rogue waves have not only been observed in continuous media but have also been reported in discrete systems, such as the systems of the well-known Ablowitz-Ladik (A-L) equation [52].

Though the rogue waves have been reported in different branches of physics where the system dynamics is governed by single equation, to the best our knowledge, they have been observed and reported very little in the coupled systems. For example, Rogue waves of the coupled NLS were constructed in the literatures [53–55]. Very recently, new kinds of matter rogue waves [56] have been reported in  $F = 1$  spinor Bose-Einstein condensate

system controlled by three component NLS equation. In experiment, the rogue waves in a multistable system [57] is revealed by experiments with an erbium-doped fiber laser driven by harmonic pump modulation. So, it is our prime interest to analyze the possibility of rogue waves in coupled systems, such as NLS-MB system.

It is well known that the dark soliton [58] of the defocusing nonlinear Schrödinger (NLS) equation is essentially different from that of bright soliton. For the past two decades or so, intensive research have been carried by several groups about theoretical and experimental aspects of dark bright solitons, it is quite natural to ask a question: is there any possibility of observing dark rogue wave in soliton equations? In general, the first order dark rogue wave has one down dominant peak and two small lumps. Because of the singularity [17, 18] of the solution for the de-focusing NLS equation generated by using DT, we cannot get dark rogue wave of the de-focusing by this way. Fortunately, we have obtained dark and bright rogue waves [59] of the NLS-MB equations from a Taylor series expansion of the first order breather solutions, which are generated from a periodic seed by the DT. But we did not provide a detailed analysis on their dynamical evolution and higher order rogue waves. The aim of this paper is twofold. Firstly, the determinant representation of the  $n$ -fold DT of the NLS-MB equations are similar to the case of NLS equation DT [60]. Secondly, the rogue waves of the three optical fields are constructed by determinant forms. It should be noted that the rogue waves of the fields  $p$  and  $\eta$  are dark. Furthermore, the connection between our rogue waves and the generation of supercontinuum generation will be discussed.

The organization of this paper is as follows. In section 2, the determinant representation of the  $n$ -fold DT and formulae of  $E^{[n]}$ ,  $p^{[n]}$  and  $\eta^{[n]}$  are expressed by eigenfunctions of spectral problem. In section 3, a Taylor series expansion about the breather solutions are generated by  $n$ -fold DT from a periodic seed solution with a constant amplitude to construct the bright and dark rogue waves. What is more, the  $n$ -order rogue waves are given by determinant forms with  $n + 3$  free parameters. Finally, we conclude the results in section 4.

## II. DARBOUX TRANSFORMATION

The linear spectral problem of the NLS-MB equations can be expressed as [4]

$$\Psi_x = U\Psi, \quad (3)$$

$$\Psi_t = V\Psi, \quad (4)$$

where

$$\begin{aligned}\Psi &= \begin{pmatrix} \Psi_1 \\ \Psi_2 \end{pmatrix}, \\ U &= \begin{bmatrix} \lambda & E \\ -E^* & -\lambda \end{bmatrix} \equiv \lambda\sigma_3 + U_0, \\ V &= i \left( \begin{bmatrix} 1 & 0 \\ 0 & -1 \end{bmatrix} \lambda^2 + \begin{bmatrix} 0 & E \\ -E^* & 0 \end{bmatrix} \lambda + \frac{1}{2} \begin{bmatrix} |E|^2 & E_x \\ E_x^* & -|E|^2 \end{bmatrix} \right) + \frac{1}{\lambda - i\omega_0} \begin{pmatrix} \eta & -p \\ -p^* & -\eta \end{pmatrix} \\ &\equiv i\sigma_3\lambda^2 + i\lambda V_1 + \frac{i}{2}V_0 + \frac{1}{\lambda - i\omega_0}V_{-1},\end{aligned}$$

and  $\lambda$  is the complex eigenvalue parameter. It is easy to prove that the spectral problem (3) and (4) are transformed to

$$\Psi^{[1]}_x = U^{[1]} \Psi^{[1]}, \quad U^{[1]} = (T_x + T U)T^{-1}, \quad (5)$$

$$\Psi^{[1]}_t = V^{[1]} \Psi^{[1]}, \quad V^{[1]} = (T_t + T V)T^{-1}, \quad (6)$$

under a gauge transformation

$$\Psi^{[1]} = T \Psi. \quad (7)$$

Here,  $T$  is a  $2 \times 2$  matrix, which is determined by the cross differentiating (5) and (6),

$$U^{[1]}_t - V^{[1]}_x + [U^{[1]}, V^{[1]}] = T(U_t - V_x + [U, V])T^{-1}. \quad (8)$$

This implies that, in order to make eq.(3) and eq.(4) invariant under the transformation (7), it is crucial to search a matrix  $T$  such that  $U^{[1]}$  and  $V^{[1]}$  have the same forms as  $U$  and  $V$ . At the same time the old potential (or seed solutions)  $(E, p, \eta)$  in spectral matrixes  $U$  and  $V$  are mapped into new potentials (or new solutions)  $(E^{[1]}, p^{[1]}, \eta^{[1]})$  in terms of new spectral matrixes  $U^{[1]}$  and  $V^{[1]}$ .

**2.1 One-fold Darboux transformation of NLS-MB equations**

In order to be self-contained, we shall recall the one-fold DT[16] of NLS-MB equations. Considering the application of the representation for the n-fold DT by means of the determinant[60] of eigenfunctions with different eigenvalues in the following context, we need to introduce  $2n$  eigenfunctions by  $f_k = f_k(\lambda_k) = \begin{pmatrix} f_{k1} \\ f_{k2} \end{pmatrix}$  associated with an eigenvalue  $\lambda_k$ , and  $\lambda_k = \lambda_m$  if  $k = m$ , where  $k = 1, 2, 3, \dots, 2n$  but  $\lambda_k \neq \lambda$ . Additionally, the eigenfunctions for distinct eigenvalues are linearly independent, (i.e.)  $f_k$  and  $f_m$  are linearly independent if  $k \neq m$ .

The elements of one-fold DT [16] are parameterized by the eigenfunction  $f_k$  associated with  $\lambda_k$  as

$$T_1(\lambda; \lambda_1, \lambda_2) = \lambda I + S = \begin{pmatrix} \frac{\widetilde{(T_1)_{11}}}{|W_2|} & \frac{\widetilde{(T_1)_{12}}}{|W_2|} \\ \frac{\widetilde{(T_1)_{21}}}{|W_2|} & \frac{\widetilde{(T_1)_{22}}}{|W_2|} \end{pmatrix}, \quad (9)$$

Here  $I$  is a unit matrix, and

$$S = \begin{pmatrix} \frac{\begin{vmatrix} -\lambda_1 f_{11} & f_{12} \\ -\lambda_2 f_{21} & f_{22} \end{vmatrix}}{|W_2|} & \frac{\begin{vmatrix} f_{11} & -\lambda_1 f_{11} \\ f_{21} & -\lambda_2 f_{21} \end{vmatrix}}{|W_2|} \\ \frac{\begin{vmatrix} -\lambda_1 f_{12} & f_{12} \\ -\lambda_2 f_{22} & f_{22} \end{vmatrix}}{|W_2|} & \frac{\begin{vmatrix} f_{11} & -\lambda_1 f_{12} \\ f_{21} & -\lambda_2 f_{22} \end{vmatrix}}{|W_2|} \end{pmatrix},$$

$$W_2(f_1, f_2) = \begin{pmatrix} f_{11} & f_{12} \\ f_{21} & f_{22} \end{pmatrix}, \quad \det(T_1) = (\lambda - \lambda_1)(\lambda - \lambda_2),$$

$$\widetilde{(T_1)_{11}} = \begin{vmatrix} 1 & 0 & \lambda \\ f_{11} & f_{12} & \lambda_1 f_{11} \\ f_{21} & f_{22} & \lambda_2 f_{21} \end{vmatrix}, \quad \widetilde{(T_1)_{12}} = \begin{vmatrix} 0 & 1 & 0 \\ f_{11} & f_{12} & \lambda_1 f_{11} \\ f_{21} & f_{22} & \lambda_2 f_{21} \end{vmatrix},$$

$$\widetilde{(T_1)_{21}} = \begin{vmatrix} 1 & 0 & 0 \\ f_{11} & f_{12} & \lambda_1 f_{12} \\ f_{21} & f_{22} & \lambda_2 f_{22} \end{vmatrix}, \quad \widetilde{(T_1)_{22}} = \begin{vmatrix} 0 & 1 & \lambda \\ f_{11} & f_{12} & \lambda_1 f_{12} \\ f_{21} & f_{22} & \lambda_2 f_{22} \end{vmatrix}.$$

With the transformed potentials,

$$\begin{aligned}U_0^{[1]} &= U_0 - [\sigma_3, T_1], \\ V_{-1}^{[1]} &= T_1|_{\lambda=i\omega_0} V_{-1} T_1^{-1}|_{\lambda=i\omega_0},\end{aligned} \quad (10)$$

The resulting new solutions of  $E^{[1]}$ ,  $p^{[1]}$  and  $\eta^{[1]}$  are given by

$$E^{[1]} = E - 2S_{12}, \quad (11)$$

$$p^{[1]} = -\frac{1}{\det(T_1)}(-2\eta(T_1)_{11}(T_1)_{12} + p^*(T_1)_{12}(T_1)_{12} - p(T_1)_{11}(T_1)_{11})|_{\lambda=i\omega_0}, \quad (12)$$

$$\eta^{[1]} = \frac{1}{\det(T_1)}(\eta((T_1)_{11}(T_1)_{22} + (T_1)_{12}(T_1)_{21}) - p^*(T_1)_{12}(T_1)_{22} + p(T_1)_{11}(T_1)_{21})|_{\lambda=i\omega_0}, \quad (13)$$

and the new eigenfunction  $f_k^{[1]}$  of  $\lambda_k$  corresponding to the new potentials is

$$f_k^{[1]} = \begin{pmatrix} \begin{array}{ccc} f_{k1} & f_{k2} & \lambda_k f_{k1} \\ f_{11} & f_{12} & \lambda_1 f_{11} \\ f_{21} & f_{22} & \lambda_2 f_{21} \end{array} \\ \hline |W_2| \\ \begin{array}{ccc} f_{k1} & f_{k2} & \lambda_k f_{k2} \\ f_{11} & f_{12} & \lambda_1 f_{12} \\ f_{21} & f_{22} & \lambda_2 f_{22} \end{array} \\ \hline |W_2| \end{pmatrix}.$$

In order to satisfy the constraints of  $S'$  and  $V'_{-1}$  in [16], set

$$\lambda_2 = -\lambda_1^*, f_2 = \begin{pmatrix} -f_{12}^* \\ f_{11}^* \end{pmatrix}. \quad (14)$$

## 2.2 n-fold Darboux transformation for NLS-MB equations

In this subsection, our prime aim is to establish the determinant representation of the n-fold DT for NLS-MB equations as we have done for the case of NLS equation[60]. According to the form of  $T_1$  in eq.(9), the n-fold DT should be of the form  $T_n = T_n(\lambda) = \lambda^n I + t_1 \lambda^{n-1} + t_2 \lambda^{n-2} + \dots + t_{n-1} \lambda + t_n$ , where  $t_i$  are  $2 \times 2$  matrices,  $i = 1, 2, \dots, n$ .  $T_n$  which leads to the determinant representation of  $T_n$  by means of its kernel. Specifically, from algebraic equations,

$$\begin{aligned} f_k^{[n]} &= T_n(\lambda; \lambda_1, \lambda_2, \dots, \lambda_{2n-1}, \lambda_{2n})|_{\lambda=\lambda_i} f_k = \\ &\sum_{l=0}^n t_l \lambda_k^l f_k = 0, i = 1, 2, \dots, 2n-1, 2n, \end{aligned} \quad (15)$$

with

$$t_0 = \begin{pmatrix} 1 & 0 \\ 0 & 1 \end{pmatrix},$$

coefficients  $t_l, l = 1, 2, \dots, n$  are solved by Cramer's rule. Thus we obtain the determinant representation of the  $T_n$ .

**Theorem 1.** The n-fold DT of the NLS-MB equations is  $T_n = T_n(\lambda) = \lambda^n I + t_1 \lambda^{n-1} + t_2 \lambda^{n-2} + \dots + t_{n-1} \lambda + t_n$ , where  $t_i$  are  $2 \times 2$  matrices,  $i = 1, 2, \dots, n$ . The final form of  $T_n(\lambda)$  has the form,

$$T_n = T_n(\lambda; \lambda_1, \lambda_2, \dots, \lambda_{2n-1}, \lambda_{2n}) = \begin{pmatrix} \frac{\widetilde{(T_n)_{11}}}{|W_{2n}|} & \frac{\widetilde{(T_n)_{12}}}{|W_{2n}|} \\ \frac{\widetilde{(T_n)_{21}}}{|W_{2n}|} & \frac{\widetilde{(T_n)_{22}}}{|W_{2n}|} \end{pmatrix}, \quad (16)$$

Here  $I$  is a unit matrix, and expression for  $t_1$  and components of  $T_n$  are given in Appendix I

It is easy to construct a simple form of the determinant of  $T_n$

$$\det(T_n) = (\lambda - \lambda_1)(\lambda - \lambda_2) \cdots (\lambda - \lambda_{2n-1})(\lambda - \lambda_{2n})$$

Next, we consider the transformed new solutions  $(E^{[n]}, p^{[n]}, \eta^{[n]})$  of NLS-MB equations corresponding to the n-fold DT.

**Corollary] 1.** For the n-fold DT, the transformed potentials are

$$\begin{aligned} U_0^{[n]} &= U_0 - [\sigma_3, T_n], \\ V_{-1}^{[n]} &= T_n|_{\lambda=i\omega_0} V_{-1} T_n^{-1}|_{\lambda=i\omega_0}, \end{aligned} \quad (17)$$

which leads to the new solutions  $E^{[n]}, p^{[n]}$  and  $\eta^{[n]}$  of the form

$$E^{[n]} = E - 2(t_1)_{12}, \quad (18)$$

$$p^{[n]} = -\frac{1}{\det(T_n)}(-2\eta(T_n)_{11}(T_n)_{12} + p^*(T_n)_{12}(T_n)_{12} - p(T_n)_{11}(T_n)_{11})|_{\lambda=i\omega_0}, \quad (19)$$

$$\eta^{[n]} = \frac{1}{\det(T_n)}(\eta(T_n)_{11}(T_n)_{22} + (T_n)_{12}(T_n)_{21}) - p^*(T_n)_{12}(T_n)_{22} + p(T_n)_{11}(T_n)_{21})|_{\lambda=i\omega_0}, \quad (20)$$

and the new eigenfunction  $f_k^{[n]}$  of  $\lambda_k$  is

$$f_k^{[n]} = \left( \begin{array}{c} \left| \begin{array}{cccccccccc} f_{k1} & f_{k2} & \lambda_k f_{k1} & \lambda_k f_{k2} & \lambda_k^2 f_{k1} & \lambda_k^2 f_{k2} & \dots & \lambda_k^{n-1} f_{k1} & \lambda_k^{n-1} f_{k2} & \lambda_k^n f_{k1} \\ f_{11} & f_{12} & \lambda_1 f_{11} & \lambda_1 f_{12} & \lambda_1^2 f_{11} & \lambda_1^2 f_{12} & \dots & \lambda_1^{n-1} f_{11} & \lambda_1^{n-1} f_{12} & \lambda_1^n f_{11} \\ f_{21} & f_{22} & \lambda_2 f_{21} & \lambda_2 f_{22} & \lambda_2^2 f_{21} & \lambda_2^2 f_{22} & \dots & \lambda_2^{n-1} f_{21} & \lambda_2^{n-1} f_{22} & \lambda_2^n f_{21} \\ f_{31} & f_{32} & \lambda_3 f_{31} & \lambda_3 f_{32} & \lambda_3^2 f_{31} & \lambda_3^2 f_{32} & \dots & \lambda_3^{n-1} f_{31} & \lambda_3^{n-1} f_{32} & \lambda_3^n f_{31} \\ \vdots & \vdots & \vdots & \vdots & \vdots & \vdots & \vdots & \vdots & \vdots & \vdots \\ f_{2n1} & f_{2n2} & \lambda_{2n} f_{2n1} & \lambda_{2n} f_{2n2} & \lambda_{2n}^2 f_{2n1} & \lambda_{2n}^2 f_{2n2} & \dots & \lambda_{2n}^{n-1} f_{2n1} & \lambda_{2n}^{n-1} f_{2n2} & \lambda_{2n}^n f_{2n1} \end{array} \right| \\ \hline \left| \begin{array}{cccccccccc} f_{k1} & f_{k2} & \lambda_k f_{k1} & \lambda_k f_{k2} & \lambda_k^2 f_{k1} & \lambda_k^2 f_{k2} & \dots & \lambda_k^{n-1} f_{k1} & \lambda_k^{n-1} f_{k2} & \lambda_k^n f_{k2} \\ f_{11} & f_{12} & \lambda_1 f_{11} & \lambda_1 f_{12} & \lambda_1^2 f_{11} & \lambda_1^2 f_{12} & \dots & \lambda_1^{n-1} f_{11} & \lambda_1^{n-1} f_{12} & \lambda_1^n f_{12} \\ f_{21} & f_{22} & \lambda_2 f_{21} & \lambda_2 f_{22} & \lambda_2^2 f_{21} & \lambda_2^2 f_{22} & \dots & \lambda_2^{n-1} f_{21} & \lambda_2^{n-1} f_{22} & \lambda_2^n f_{22} \\ f_{31} & f_{32} & \lambda_3 f_{31} & \lambda_3 f_{32} & \lambda_3^2 f_{31} & \lambda_3^2 f_{32} & \dots & \lambda_3^{n-1} f_{31} & \lambda_3^{n-1} f_{32} & \lambda_3^n f_{32} \\ \vdots & \vdots & \vdots & \vdots & \vdots & \vdots & \vdots & \vdots & \vdots & \vdots \\ f_{2n1} & f_{2n2} & \lambda_{2n} f_{2n1} & \lambda_{2n} f_{2n2} & \lambda_{2n}^2 f_{2n1} & \lambda_{2n}^2 f_{2n2} & \dots & \lambda_{2n}^{n-1} f_{2n1} & \lambda_{2n}^{n-1} f_{2n2} & \lambda_{2n}^n f_{2n2} \end{array} \right| \\ \hline |W_{2n}| \end{array} \right).$$

Note that

$$\lambda_{2k} = -\lambda_{2k-1}^*, f_{2k} = \begin{pmatrix} -f_{2k-12}^* \\ f_{2k-11}^* \end{pmatrix} \quad (21)$$

in order to satisfy the constraints of DT.

ated by assuming a periodic seed solution. Then we can construct the explicit bright and dark rogue waves of the NLS-MB equations through a Taylor series expansion of the breather solutions.

### III. N-ORDER BRIGHT AND DARK ROGUE WAVES GENERATED BY N-ORDER BREATHER SOLUTIONS

By using the results of DT discussed above, breather solutions of  $E$ ,  $p$  and  $\eta$  of NLS-MB equations are gener-

Substituting,  $E = d \exp[i\rho]$ ,  $p = ifE$ ,  $\eta = 1$  into the spectral problem eq.(3) and eq.(4), and using the method of separation of variables and the superposition principle, the eigenfunction  $f_{2k-1}$  associated with  $\lambda_{2k-1}$  is given by

$$\begin{pmatrix} f_{2k-11}(x, t, \lambda_{2k-1}) \\ f_{2k-12}(x, t, \lambda_{2k-1}) \end{pmatrix} = \begin{pmatrix} C_1 \varpi(x, t, \lambda_{2k-1})[1, 2k-1] - C_2 \varpi^*(x, t, -\lambda_{2k-1}^*)[2, 2k-1] \\ C_1 \varpi(x, t, \lambda_{2k-1})[2, 2k-1] + C_2 \varpi^*(x, t, -\lambda_{2k-1}^*)[1, 2k-1] \end{pmatrix}. \quad (22)$$

Here

$$\begin{pmatrix} \varpi(x, t, \lambda_{2k-1})[1, 2k-1] \\ \varpi(x, t, \lambda_{2k-1})[2, 2k-1] \end{pmatrix} = \begin{pmatrix} d \exp\left[\frac{i}{2}\rho + ic(\lambda_{2k-1})\right] \\ \left[ i(c_1(\lambda_{2k-1}) + \frac{b}{2}) - \lambda_{2k-1} \right] \exp\left[-\frac{i}{2}\rho + ic(\lambda_{2k-1})\right] \end{pmatrix},$$

$$\varpi(x, t, \lambda_{2k-1}) = \begin{pmatrix} \varpi(x, t, \lambda_{2k-1})[1, 2k-1] \\ \varpi(x, t, \lambda_{2k-1})[2, 2k-1] \end{pmatrix}.$$

Note that  $\varpi(x, t, \lambda_{2k-1})$  is the basic solution of the spectral problem eq.(3) and eq.(4). Here  $a, b, d, t, z \in \mathbb{R}$ ,

$C_1, C_2 \in \mathbb{C}$ ,

$$\begin{aligned} c(\lambda_{2k-1}) &= c_1(\lambda_{2k-1})x + c_2(\lambda_{2k-1})t, \\ c_1(\lambda_{2k-1}) &= \sqrt{d^2 - \left(\frac{ib}{2} - \lambda_{2k-1}\right)^2}, \\ c_2(\lambda_{2k-1}) &= \left(i\lambda_{2k-1} - \frac{b}{2} - \frac{if}{\lambda_{2k-1} - i\omega_0}\right) c_1(\lambda_{2k-1}), \\ \rho &= a t + b x, \\ f &= \frac{1}{2}(a + \frac{b^2}{2} - d^2), \end{aligned}$$

and the  $(-b + 2\omega_0)f = 2$  is used for  $f$ .

3.1 The n-order breather solutions of NLS-MB equa-

tions

For simplicity, under the condition  $C_1 = C_2 = 1$ , let  $\lambda_{2k-1} = \alpha_{2k-1} + i\frac{b}{2}$ , such that  $\text{Im}\left(\frac{ib}{2} - \lambda_{2k-1}\right) = 0$  and  $c_1(\lambda_{2k-1}) = \sqrt{d^2 - \text{Re}^2(\lambda_{2k-1})} \in \mathbb{R}$ , and using eq. (21), then substituting eigenfunctions eq. (22) into eq. (16), we obtain the determinant representation of DT in the form which is discussed in Appendix II.

Using eq. (A.1) into eq.(18,19,20) with the choice in eq.(A.2), we can construct  $E^{[n]}, p^{[n]}$  and  $\eta^{[n]}$ . For brevity, in the following, we are giving only an explicit expression of  $E^{[1]}$  with specific parameters  $d = 1, b = 2, \omega_0 = \frac{1}{2}$ .

$$\begin{aligned} E^{[1]} &= E + 4\alpha_1 \frac{v_3}{v_4} \exp(i(-5t + 2x)), \\ v_3 &= -\alpha_1 \cos(2w_1) + (2 \cos(w_1) + 2\sqrt{1 - \alpha_1^2} \sin(w_1)\alpha_1 + 2\alpha_1^2 \cos(w_1)) \cosh(w_2) \\ &\quad + (2i\alpha_1^2 \sin(w_1) - 2i \sin(w_1) - 2i\alpha_1 \cos(w_1)\sqrt{1 - \alpha_1^2}) \sinh(w_2) - 2\alpha_1 - \sqrt{1 - \alpha_1^2} \sin(2w_1) \\ &\quad + i\sqrt{1 - \alpha_1^2} \sinh(2w_2) - \alpha_1 \cosh(2w_2), \\ v_4 &= 2\alpha_1^2 \cos(2w_1) - 2(4\alpha_1 \cos(w_1) + 2 \sin(w_1)\sqrt{1 - \alpha_1^2}) \cosh(w_2) \\ &\quad - 2(-1 - \alpha_1^2 - \cosh(2w_2) - \sqrt{1 - \alpha_1^2}\alpha_1 \sin(2w_1)), \\ w_1 &= -2\sqrt{1 - \alpha_1^2}x + \frac{12}{5}\sqrt{1 - \alpha_1^2}t, w_2 = \frac{26}{5}\sqrt{1 - \alpha_1^2}t. \end{aligned}$$

The dynamical evolution of  $|E^{[1]}|^2$ ,  $|p^{[1]}|^2$  and  $\eta^{[1]}$  for the parametric choice  $d = 1, b = 2, \omega_0 = \frac{1}{2}, \alpha_1 = 0.8$  are plotted in the Figures 1-3, which confirms the direct verification of the periodic as well as decaying properties of typical breather solutions. The breather of  $E^{[1]}$  is almost same as that of the NLS equation, which has one upper peak and two caves in each periodic unit. On the other hand, we observe that there are two new kinds of breathers for  $p^{[1]}$  and  $\eta^{[1]}$ . It is interesting to note that new breather  $p^{[1]}$  admit one upper ring and three down peaks in each periodic unit. Whereas the new breather  $\eta^{[1]}$  has two lumps and one down peak in each periodic unit. Moreover, these two new breathers can be called as dark breathers because the down amplitude is dominant in both the cases. The above discussed new properties are clearly seen in Figures 1-3.

3.2 The first-order rogue waves generated by first-order breather solutions above

Similarly, under the condition  $C_1 = C_2 = 1$ , substituting eigenfunctions eq.(22) into eqs.(18,19,20) with  $\lambda_1 = \alpha_1 + i\frac{b}{2}$ , by assuming  $\alpha_1 \rightarrow d(d > 0)$ ,  $E^{[1]}, p^{[1]}$  and  $\eta^{[1]}$  become rational solutions  $\{\tilde{E}^{[1]}, \tilde{p}^{[1]}, \tilde{\eta}^{[1]}\}$  in the form of rogue waves [59]. When  $x \rightarrow \infty, t \rightarrow \infty$  in the

above expressions, after some manipulations, we find  $|\tilde{E}^{[1]}|^2 \rightarrow d^2, |\tilde{p}^{[1]}|^2 \rightarrow \frac{d^2}{(\frac{b}{2} - \omega_0)^2}$  and  $\tilde{\eta}^{[1]} \rightarrow 1$ . In

addition to the above conditions, from  $|\tilde{E}^{[1]}|_x^2 = 0$  and  $|\tilde{E}^{[1]}|_t^2 = 0$ , we also observe that the maximum amplitude of  $|\tilde{E}^{[1]}|^2$  occurs at  $t = 0$  and  $x = 0$  and is equal to  $9d^2$ , and the minimum amplitude of  $|\tilde{E}^{[1]}|^2$  occurs at  $t = 0$  and  $x = \pm \frac{\sqrt{3}}{2d}$  and is equal to 0. By using similar procedure discussed above, we can also obtain the extreme value of  $|\tilde{p}^{[1]}|^2$  and  $\tilde{\eta}^{[1]}$ .

Figure 4 is plotted for the rogue wave  $|\tilde{E}^{[1]}|^2$  with specific parameters  $d = 1, b = 2, \omega_0 = \frac{1}{2}$ . From figure 4, we infer the following interesting results: 1) the  $|\tilde{E}^{[1]}|^2 \rightarrow 1$  by assuming  $x \rightarrow \infty, t \rightarrow \infty$  which gives the asymptotic plane; 2) The maximum amplitude of  $|\tilde{E}^{[1]}|^2$  occurs at  $t = 0$  and  $x = 0$  and is equal to 9, and the minimum amplitude of  $|\tilde{E}^{[1]}|^2$  occurs at  $t = 0$  and  $x = \pm \frac{\sqrt{3}}{2}$  and is equal to 0. As the general expression of the extreme values of  $|p^{[1]}|^2$  and  $\tilde{\eta}^{[1]}$  are quite complicated in nature, for simplicity, we only discuss these solutions under certain choice of parameters.

Figure 5 is plotted for the rogue wave  $|\tilde{p}^{[1]}|^2$  on  $(x - t)$

plane with the above parameters. Like in the earlier case, here also we observe the following salient features: 1) the height of the asymptotical plane is 4 because  $|\bar{p}^{[1]}|^2 \rightarrow 4$ , when  $x \rightarrow \infty$ ,  $t \rightarrow \infty$ ; 2) The maximum amplitude of  $|\bar{p}^{[1]}|^2$  occurs in the form of ring curve on  $(x-t)$  plane defined by  $-\frac{507}{16}t^2 + \frac{1681}{8}t^4 + \frac{25}{8}x^4 - \frac{55}{128} + \frac{65}{16}x^2 + \frac{277}{4}x^2t^2 - 15x^3t + \frac{65}{4}xt - 123xt^3 = 0$ , and is equal to 5, and the minimum amplitude of  $|\bar{p}^{[1]}|^2$  occurs at four points  $\{(t = \frac{+5 + \sqrt{5}}{52}, x = \frac{+19 + 9\sqrt{5}}{52}), (t = \frac{+5 - \sqrt{5}}{52}, x = \frac{+19 - 9\sqrt{5}}{52}), (t = \frac{-5 + \sqrt{5}}{52}, x = \frac{-19 + 9\sqrt{5}}{52}), (t = \frac{-5 - \sqrt{5}}{52}, x = \frac{-19 - 9\sqrt{5}}{52})\}$  and is equal to 0; 3) the extreme value of the amplitude  $|\bar{p}^{[1]}|^2$  occurs at  $t = 0$  and  $x = 0$  and is equal to  $\frac{4}{25}$ . We also observe that the middle down peak in Figure 5 has two sub-peaks. Due to the direction of the observation of the figure, these two close sub-peaks are not clearly distinguished from the figure, we just find three down peaks.

Figure 6 is plotted for the rogue wave  $\tilde{\eta}^{[1]}$  with specific parameters as in fig.4. From the Figure, we observe the following new results: 1) the height of the asymptotical plane is 1 because  $\tilde{\eta}^{[1]} \rightarrow 1$  by letting  $x \rightarrow \infty$ ,  $t \rightarrow \infty$ ; 2) the maximum amplitude of  $\tilde{\eta}^{[1]}$  occurs at two points  $\{(t = \frac{5 + \sqrt{5}}{52}, x = \frac{19 + 9\sqrt{5}}{52})\}$  and  $\{(t = \frac{5 + \sqrt{5}}{52}, x = \frac{19 + 9\sqrt{5}}{52})\}$  and is equal to  $\sqrt{5}$ , and the minimum amplitude of  $\tilde{\eta}^{[1]}$  occurs at two points  $\{(t = \frac{+5 - \sqrt{5}}{52}, x = \frac{+19 - 9\sqrt{5}}{52})\}$  and  $\{(t = \frac{-5 + \sqrt{5}}{52}, x = \frac{-19 + 9\sqrt{5}}{52})\}$  and is equal to  $-\sqrt{5}$ ;

3) the extreme value of the amplitude  $\tilde{\eta}^{[1]}$  occurs at  $t = 0$  and  $x = 0$  and is equal to  $-\frac{11}{5}$ . Like in Figure.5, here also we observe that the down peak in Figure 6 has two sub-peaks.

### 3.3 The higher order rogue waves and their determinant forms

In order to emphasize the richness of the higher order rogue waves, we can modify  $C_1$  and  $C_2$  in the equation (22) as the following:

$$\begin{aligned} C_1 &= K_0 + \exp(ic_1(\lambda_{2k-1}) \sum_{j=0}^{k-1} J_j (\lambda_{2k-1} - (d + i\frac{b}{2}))^j) \\ C_2 &= K_0 + \exp(-ic_1(\lambda_{2k-1}) \sum_{j=0}^{k-1} J_j (\lambda_{2k-1} - (d + i\frac{b}{2}))^j) \end{aligned} \quad (23)$$

Here  $K_0, J_j \in \mathbb{C}$ . Note that  $\lambda_{2k-1} = d + i\frac{b}{2}$  is the zero point of  $c_1(\lambda_{2k-1})$ .

Based on the section 3.2, higher order rogue waves can be constructed by the breather solutions. In other words, let  $\lambda_{2k-1} \rightarrow d + i\frac{b}{2}$  in n-order breather solutions, n-order rogue waves can be given. Generally, in comparison to the method of limiting the breather solutions, the method of making rational eigenfunction below may be more direct and the rogue wave can be shown by determinant forms.

Substituting eq.(23) into eqs.(22), by assuming  $\lambda_{2k-1} \rightarrow d + i\frac{b}{2}$ , eigenfunction  $f_{2k-1}$  associated with  $\lambda_{2k-1}$  become rational eigenfunction  $f_r$  as follows.

$$\begin{pmatrix} f_{r1} \\ f_{r2} \end{pmatrix} = \begin{pmatrix} -(2dK_0 + 2d)x + 2\left(\frac{2i}{(b-2\omega_0)(d + \frac{1}{2}ib - i\omega_0)} + id - b\right)(K_0 + 1)dt + 2J_0d + K_0 + 1 \sqrt{2d} \exp(K) \\ -(2dK_0 + 2d)x - 2\left(\frac{2i}{(b-2\omega_0)(d + \frac{1}{2}ib - i\omega_0)} + id - b\right)(K_0 + 1)dt - 2J_0d + K_0 + 1 \sqrt{2d} \exp(-K) \end{pmatrix},$$

$$K = \frac{1}{2}i\left(-\frac{8 + b^3 - 2b^2\omega_0 - 2d^2b + 4d^2\omega_0}{2(b-2\omega_0)}t + bx\right) \quad (24)$$

Substituting eigenfunctions eq.(24) into eqs.(11,12,13), we can get the first order rogue waves  $\{\bar{E}^{[1]}, \bar{p}^{[1]}, \tilde{\eta}^{[1]}\}$  in the form of determinant. The dynamical evolution of  $|\bar{E}^{[1]}|^2$ ,  $|\bar{p}^{[1]}|^2$  and  $\tilde{\eta}^{[1]}$  for the parametric choice

$d, b, \omega_0, K_0, J_0$  are respectively similar to the Figures 4-6, but we can control the position of the first-order rogue waves by choosing the parameters  $K_0$  and  $J_0$ .

**Theorem 2.** For the n-fold DT, the n-order rogue waves

$\bar{E}^{[n]}$ ,  $\bar{p}^{[n]}$  and  $\bar{\eta}^{[n]}$  of the form

$$\bar{E}^{[n]} = E - 2(\bar{t}_{r1})_{12}, \quad (25)$$

$$\bar{p}^{[n]} = -\frac{1}{\det(\bar{T}_{rn})}(-2\eta(\bar{T}_{rn})_{11}(\bar{T}_{rn})_{12} + p^*(\bar{T}_{rn})_{12}(\bar{T}_{rn})_{12} - p(\bar{T}_{rn})_{11}(\bar{T}_{rn})_{11})|_{\lambda=i\omega_0}, \quad (26)$$

$$\bar{\eta}^{[n]} = \frac{1}{\det(\bar{T}_{rn})}(\eta((\bar{T}_{rn})_{11}(\bar{T}_{rn})_{22} + (\bar{T}_{rn})_{12}(\bar{T}_{rn})_{21}) - p^*(\bar{T}_{rn})_{12}(\bar{T}_{rn})_{22} + p(\bar{T}_{rn})_{11}(\bar{T}_{rn})_{21})|_{\lambda=i\omega_0}, \quad (27)$$

The final form of  $\bar{T}_{rn}(\lambda)$  is given in Appendix III.

**Case 1).** When  $n = 2$ , substituting eq.(B.1) into eq.(25), eq.(26) and eq.(27) can give the second-order rogue waves with five free parameters. Note that under the condition  $J_1 \gg J_0$ , the second-rogue can split into three first-order rogue wave (triplets rogue wave) [61] rather than two. The dynamical evolution of  $|\bar{E}^{[2]}|^2$ ,  $|\bar{p}^{[2]}|^2$  and  $\bar{\eta}^{[2]}$  for the parametric choice  $d = 1, b = 2, \omega_0 = \frac{1}{2}, K_0 = 1, J_0 = 0, J_1 = 100$  are plotted in the Figures 7, 9 and 11 and their corresponding density plots are shown in the Figures 8, 10 and 12. There is another kind of second-order rogue wave, for example,  $|\bar{E}^{[2]}|^2$  is higher than second-rogue above. The dynamical evolution of  $|\bar{E}^{[2]}|^2$ ,  $|\bar{p}^{[2]}|^2$  and  $\bar{\eta}^{[2]}$  for the parametric choice  $d = 2, b = 0, \omega_0 = \frac{1}{2}, K_0 = 1, J_0 = 0, J_1 = 0$  are plotted in the Figures 13-15. Note that eigenvalue  $\lambda_1 = \lambda_3$  is real. The eigenvalue of rogue waves are different from the eigenvalue of solutions given in the past.

**Case 2).** When  $n = 3$ , substituting eq.(B.1) into eq.(25), eq.(26) and eq.(27) can give the third-order rogue waves with six free parameters. Note that under the condition  $J_2 \gg J_i (i = 0, 1)$  or  $J_1 \gg J_i (i = 0, 2)$ , the third-rogue can split into six first-order rogue wave rather. Circular rogue wave [62] may be constructed by the condition  $J_2 \gg J_1$  and  $J_2 \gg J_0$ . The dynamical evolution of  $|\bar{E}^{[3]}|^2$ ,  $|\bar{p}^{[3]}|^2$  and  $\bar{\eta}^{[3]}$  for the parametric choice  $d = 1, b = 2, \omega_0 = \frac{1}{2}, K_0 = 1, J_0 = 0, J_1 = 0, J_2 = 8000$  are plotted in the Figures 16-18. At the same time, triplets rogue wave may be constructed by the condition  $J_1 \gg J_2$  and  $J_1 \gg J_0$ . The dynamical evolution of  $|\bar{E}^{[3]}|^2$ ,  $|\bar{p}^{[3]}|^2$  and  $\bar{\eta}^{[3]}$  for the parametric choice  $d = 1, b = 2, \omega_0 = \frac{1}{2}, K_0 = 1, J_0 = 0, J_1 = 100, J_2 = 0$  are plotted in the Figures 19-21. Similarly, there is another kind third-order rogue wave, for example,  $|\bar{E}^{[3]}|^2$  is higher than third-rogue above. The dynamical evolution of  $|\bar{E}^{[3]}|^2$ ,  $|\bar{p}^{[3]}|^2$  and  $\bar{\eta}^{[3]}$  for the parametric choice  $d = \frac{4}{3}, b = 0, \omega_0 = \frac{1}{2}, K_0 = 1, J_0 = 0, J_1 = 0, J_2 = 0$  are plotted in the Figures 22-24. Note that eigenvalue  $\lambda_1 = \lambda_3 = \lambda_5$  is real. The eigenvalue of rogue waves are different from the eigenvalue of solutions given in the past. According to analysis above, the n-order rogue

waves may be controlled by  $n + 3$  free parameters.

From the above discussions, it is interesting to point out that the down amplitudes are dominant in the profile of rogue waves  $\bar{p}^{[1]}$  and  $\bar{\eta}^{[1]}$ , so they are new kind of rogue waves when compared with the typical bright rogue wave  $\bar{E}^{[1]}$ , which are corresponding to the dark breathers in Figure 2 and Figure 3. So from our earlier understanding of breathers in other physical systems, we call these new type of solutions as dark rogue waves. Moreover, the dark rogue wave  $\bar{p}^{[1]}$  has one upper ring and three down peaks, and dark rogue wave  $\bar{\eta}^{[1]}$  has two lumps and one down peak. According to analysis, the n-order rogue waves must be generated by n-order breather solution.

From the detailed literature on rogue waves, to the best of our knowledge, so far only bright rogue waves have been analyzed in detail but there is little report about the dark rogue waves in physical system. In the case of bright optical rogue waves, many results have actually connected the generation of supercontinuum generation (SCG) with rogue waves[63]. In recent years, the supercontinuum white coherent source has attracted a lot of attention because of its potential applications in optical coherence tomography, spectroscopy, wavelength division multiplexing, etc. As reported in ref.[64], the modulational instability (MI) conditions for the generation of ultra-short pulses has already been investigated in the erbium doped nonlinear fibre and occurrences of nonconventional side bands have also been observed. This type of nonconventional side bands will be very useful to generate large MI bandwidth which intern generates very short pulses. In this way, we believe that our rogue wave results in this paper can also be connected to the generation of SCG. Similarly, the occurrence of dark rogue wave can also be connected to the results of ref.[64], in the following manner: In our above work[64], it has been shown that both bright and dark SIT solitons can be generated in the case of the anomalous and normal group velocity dispersion (GVD), in contrast to the well-established results in the conventional fibre, where bright and dark solitons exists in the anomalous and normal GVD regions, respectively. From the above results, it is clear that the formation of dark rogue waves can also be connected in a similar way. Thus, it is interesting to analyze the relation connecting the MI, SCG and rogue wave formation in optical system.



#### IV. CONCLUSION

Thus, in this article, we have reported the rogue waves of the three physical fields  $E, p$ , and  $\eta$  in a resonant erbium-doped fibre system, which is governed by the NLS-MB equations. These rogue waves are constructed by a Taylor series expansion of the corresponding breather solutions of the NLS-MB equations. As expected, in contrast to the usual bright rogue wave  $E$ , we observe dark rogue waves for  $p$  and  $\eta$ . The main feature of the dark rogue waves is the appearance of two (or more) dominant down peaks in its profile. In particular, there is one upper ring in the profile of the  $p$ , so it may be called as dark ring-rogue wave. The explicit form of  $\bar{E}^{[n]}$ ,  $\bar{p}^{[n]}$  and  $\bar{\eta}^{[n]}$  are given by the determinant representation of the  $n$ -fold DT. The rogue waves in previous section can also be connected to the supercontinuum generation.

As we have already described in the introduction, the singularity[17] of the solutions generated by the DT is the main constraint to generate the dark rogue waves of the defocusing NLS equation. This perhaps shows that the dark rogue wave of the defocusing NLS equation can be investigated by other way such as by means of Hirota method. From the determinant representation of the  $T_n$ , it is interesting to generate the higher order rogue waves so that the dynamical interactions of rogue waves can be analysed.

In recent years, considering variable dispersion, variable nonlinearity and variable gain/loss, the investiga-

tion of solitons in nonautonomous nonlinear evolution equation equations has also attracted a lot of attention among researchers [65–68]. For example, Serkin and his coworkers have proposed a novel method to analyse the nonautonomous soliton equations[66–68] and the interaction of solitons in variable coefficient higher order NLS equation have been investigated in detail[65]. Using the results of the above papers and making use of our results in this paper, one can also construct the multi solitons, breathers and rogue wave solutions of the variable coefficient NLS-MB system. Moreover, it is also possible to obtain new type of rogue waves for other important coupled system in optics, such as the CH-MB equations [69] and variable coefficient CH-MB equations[70, 71].

**Acknowledgments** This work is supported by the NSF of China under Grant No.10971109 and No. 11271210 and K.C.Wong Magna Fund in Ningbo University. Jingsong He is also supported the Natural Science Foundation of Ningbo under Grant No.2011A610179. KP wishes to thank the DST, DAE-BRNS, and UGC, Government of India, for the financial support through major projects. We thank Prof. Yishen Li(USTC,Hefei, China) for his useful suggestions on the rogue wave.

#### V. APPENDICES

**Appendix I:** In this appendix, we are giving expression for  $t_1$  and elements of  $T_n$

$$t_1 = \begin{pmatrix} \frac{\widetilde{(Q_n)_{11}}}{|W_{2n}|} & \frac{\widetilde{(Q_n)_{12}}}{|W_{2n}|} \\ \frac{\widetilde{(Q_n)_{21}}}{|W_{2n}|} & \frac{\widetilde{(Q_n)_{22}}}{|W_{2n}|} \end{pmatrix},$$

$$W_{2n} = \begin{pmatrix} f_{11} & f_{12} & \lambda_1 f_{11} & \lambda_1 f_{12} & \lambda_1^2 f_{11} & \lambda_1^2 f_{12} & \dots & \lambda_1^{n-1} f_{11} & \lambda_1^{n-1} f_{12} \\ f_{21} & f_{22} & \lambda_2 f_{21} & \lambda_2 f_{22} & \lambda_2^2 f_{21} & \lambda_2^2 f_{22} & \dots & \lambda_2^{n-1} f_{21} & \lambda_2^{n-1} f_{22} \\ f_{31} & f_{32} & \lambda_3 f_{31} & \lambda_3 f_{32} & \lambda_3^2 f_{31} & \lambda_3^2 f_{32} & \dots & \lambda_3^{n-1} f_{31} & \lambda_3^{n-1} f_{32} \\ \vdots & \vdots & \vdots & \vdots & \vdots & \vdots & \vdots & \vdots & \vdots \\ f_{2n1} & f_{2n2} & \lambda_{2n} f_{2n1} & \lambda_{2n} f_{2n2} & \lambda_{2n}^2 f_{2n1} & \lambda_{2n}^2 f_{2n2} & \dots & \lambda_{2n}^{n-1} f_{2n1} & \lambda_{2n}^{n-1} f_{2n2} \end{pmatrix},$$

$$\widetilde{(T_n)_{11}} = \begin{vmatrix} 1 & 0 & \lambda & 0 & \lambda^2 & 0 & \dots & \lambda^{n-1} & 0 & \lambda^n \\ f_{11} & f_{12} & \lambda_1 f_{11} & \lambda_1 f_{12} & \lambda_1^2 f_{11} & \lambda_1^2 f_{12} & \dots & \lambda_1^{n-1} f_{11} & \lambda_1^{n-1} f_{12} & \lambda_1^n f_{11} \\ f_{21} & f_{22} & \lambda_2 f_{21} & \lambda_2 f_{22} & \lambda_2^2 f_{21} & \lambda_2^2 f_{22} & \dots & \lambda_2^{n-1} f_{21} & \lambda_2^{n-1} f_{22} & \lambda_2^n f_{21} \\ f_{31} & f_{32} & \lambda_3 f_{31} & \lambda_3 f_{32} & \lambda_3^2 f_{31} & \lambda_3^2 f_{32} & \dots & \lambda_3^{n-1} f_{31} & \lambda_3^{n-1} f_{32} & \lambda_3^n f_{31} \\ \vdots & \vdots & \vdots & \vdots & \vdots & \vdots & \vdots & \vdots & \vdots & \vdots \\ f_{2n1} & f_{2n2} & \lambda_{2n} f_{2n1} & \lambda_{2n} f_{2n2} & \lambda_{2n}^2 f_{2n1} & \lambda_{2n}^2 f_{2n2} & \dots & \lambda_{2n}^{n-1} f_{2n1} & \lambda_{2n}^{n-1} f_{2n2} & \lambda_{2n}^n f_{2n1} \end{vmatrix},$$





$$\begin{aligned}
\widehat{(Q_n)}_{12} &= \begin{vmatrix} 1 & \gamma_1 & \lambda_1 & \lambda_1 \gamma_1 & \dots & \lambda_1^{n-1} & \lambda_1^n \\ -\gamma_1^* & 1 & \lambda_1^* \gamma_1^* & -\lambda_1^* & \dots & -(-\lambda_1^*)^{n-1} \gamma_1^* & -(-\lambda_1^*)^n \gamma_1^* \\ 1 & \gamma_3 & \lambda_3 & \lambda_3 \gamma_3 & \dots & \lambda_3^{n-1} & \lambda_3^n \\ \vdots & \vdots & \vdots & \vdots & \vdots & \vdots & \vdots \\ -\gamma_{2n-1}^* & 1 & \lambda_{2n-1}^* \gamma_{2n-1}^* & -\lambda_{2n-1}^* & \dots & -(-\lambda_{2n-1}^*)^{n-1} \gamma_{2n-1}^* & -(-\lambda_{2n-1}^*)^n \gamma_{2n-1}^* \end{vmatrix}, \\
\widehat{(Q_n)}_{21} &= \begin{vmatrix} 1 & \gamma_1 & \lambda_1 & \lambda_1 \gamma_1 & \lambda_1^2 & \dots & \lambda_1^{n-1} \gamma_1 & \lambda_1^n \gamma_1 \\ -\gamma_1^* & 1 & \lambda_1^* \gamma_1^* & -\lambda_1^* & -\lambda_1^{*2} \gamma_1^* & \dots & (-\lambda_1^*)^{n-1} & (-\lambda_1^*)^n \\ 1 & \gamma_3 & \lambda_3 & \lambda_3 \gamma_3 & \lambda_3^2 & \dots & \lambda_3^{n-1} \gamma_3 & \lambda_3^n \gamma_3 \\ \vdots & \vdots & \vdots & \vdots & \vdots & \vdots & \vdots & \vdots \\ -\gamma_{2n-1}^* & 1 & \lambda_{2n-1}^* \gamma_{2n-1}^* & -\lambda_{2n-1}^* & -\lambda_{2n-1}^{*2} \gamma_{2n-1}^* & \dots & (-\lambda_{2n-1}^*)^{n-1} & (-\lambda_{2n-1}^*)^n \end{vmatrix}, \\
\widehat{(Q_n)}_{22} &= \begin{vmatrix} 1 & \gamma_1 & \lambda_1 & \lambda_1 \gamma_1 & \lambda_1^2 & \dots & \lambda_1^{n-1} & \lambda_1^n \gamma_1 \\ -\gamma_1^* & 1 & \lambda_1^* \gamma_1^* & -\lambda_1^* & -\lambda_1^{*2} \gamma_1^* & \dots & -(-\lambda_1^*)^{n-1} \gamma_1^* & (-\lambda_1^*)^n \\ 1 & \gamma_3 & \lambda_3 & \lambda_3 \gamma_3 & \lambda_3^2 & \dots & \lambda_3^{n-1} & \lambda_3^n \gamma_3 \\ \vdots & \vdots & \vdots & \vdots & \vdots & \vdots & \vdots & \vdots \\ -\gamma_{2n-1}^* & 1 & \lambda_{2n-1}^* \gamma_{2n-1}^* & -\lambda_{2n-1}^* & -\lambda_{2n-1}^{*2} \gamma_{2n-1}^* & \dots & -(-\lambda_{2n-1}^*)^{n-1} \gamma_{2n-1}^* & (-\lambda_{2n-1}^*)^n \end{vmatrix}.
\end{aligned}$$

Here

$$\gamma_{2k-1} = \frac{v_1}{v_2}, \quad (\text{A.2})$$

$$\begin{aligned}
v_1 &= (2i(\alpha_{2k-1}^2 - d^2) \sin(\frac{\sqrt{d^2 - \alpha_{2k-1}^2}(-s_2x + s_4t)}{s_2}) \cos(\frac{\sqrt{d^2 - \alpha_{2k-1}^2}(-s_2x + s_4t)}{s_2}) \\
&+ i(-\alpha_{2k-1}^2 + d^2) \sin(\frac{2\sqrt{d^2 - \alpha_{2k-1}^2}(-s_2x + s_4t)}{s_2}) - 2d\alpha_{2k-1} \cosh(\frac{2\sqrt{d^2 - \alpha_{2k-1}^2}s_3t}{s_2}) \\
&+ 2d^2 \cos(\frac{2\sqrt{d^2 - \alpha_{2k-1}^2}(-s_2x + s_4t)}{s_2}) + 2id \sinh(\frac{2\sqrt{d^2 - \alpha_{2k-1}^2}s_3t}{s_2}) \sqrt{d^2 - \alpha_{2k-1}^2} \exp(-is_1), \\
v_2 &= (-2d^2 + 2\alpha_{2k-1}^2) \sinh(\frac{\sqrt{d^2 - \alpha_{2k-1}^2}s_3t}{s_2}) \cosh(\frac{\sqrt{d^2 - \alpha_{2k-1}^2}s_3t}{s_2}) + 2d^2 \cosh(\frac{2\sqrt{d^2 - \alpha_{2k-1}^2}s_3t}{s_2}) \\
&+ (d^2 - \alpha_{2k-1}^2) \sinh(\frac{2\sqrt{d^2 - \alpha_{2k-1}^2}s_3t}{s_2}) - 2\sqrt{d^2 - \alpha_{2k-1}^2}d \sin(\frac{2\sqrt{d^2 - \alpha_{2k-1}^2}(-s_2x + s_4t)}{s_2}) \\
&- 2d\alpha_{2k-1} \cos(\frac{2\sqrt{d^2 - \alpha_{2k-1}^2}(-s_2x + s_4t)}{s_2}), \\
s_1 &= \frac{-b(1/2b - \omega_0)x + (2 + 2(1/2b - \omega_0)(1/4b^2 - 1/2d^2))t}{-1/2b + \omega_0}, \\
s_2 &= (-1/2b + \omega_0)((1/2b - \omega_0)^2 + d^2), \\
s_3 &= -d\omega_0(d^2 + \omega_0^2) - 3/2db\omega_0(1/2b - \omega_0) + 1/2db(d^2 + 1/4b^2) + d, \\
s_4 &= -1/2b^2(d^2 + 1/4b^2) + b\omega_0(d^2 + \omega_0^2) + 3/2b^2\omega_0(1/2b - \omega_0) + 1/2b - \omega_0.
\end{aligned}$$

Appendix III: Here, we are giving the construction of  $\mathbf{T}$  of  $\bar{T}_{rn}(\lambda)$  in detail.

$$\bar{T}_{rn} = \bar{T}_{rn}(\lambda) = \begin{pmatrix} \widetilde{(T_{rn})_{11}} & \widetilde{(T_{rn})_{12}} \\ \widetilde{(T_{rn})_{21}} & \widetilde{(T_{rn})_{22}} \end{pmatrix}, \quad (\text{B.1})$$

$$\bar{t}_{r1} = \begin{pmatrix} \widetilde{(Q_{rn})_{11}} & \widetilde{(Q_{rn})_{12}} \\ \widetilde{(Q_{rn})_{21}} & \widetilde{(Q_{rn})_{22}} \end{pmatrix},$$

$$W_{r2n} = \begin{pmatrix} h_{01}^1 & h_{02}^1 & h_{11}^1 & h_{12}^1 & \dots & h_{n-11}^1 & h_{n-12}^1 \\ -h_{02}^{1*} & h_{01}^{1*} & h_{12}^{1*} & -h_{11}^{1*} & \dots & (-1)^n h_{n-12}^{1*} & (-1)^{n-1} h_{n-11}^{1*} \\ h_{01}^3 & h_{02}^3 & h_{11}^3 & h_{12}^3 & \dots & h_{n-11}^3 & h_{n-12}^3 \\ \vdots & \vdots & \vdots & \vdots & \vdots & \vdots & \vdots \\ -h_{02}^{2n-1*} & h_{01}^{2n-1*} & h_{12}^{2n-1*} & -h_{11}^{2n-1*} & \dots & (-1)^n h_{n-12}^{2n-1*} & (-1)^{n-1} h_{n-11}^{2n-1*} \end{pmatrix},$$

$$\widetilde{(T_{rn})_{11}} = \begin{vmatrix} 1 & 0 & \lambda & 0 & \dots & \lambda^{n-1} & 0 & \lambda^n \\ h_{01}^1 & h_{02}^1 & h_{11}^1 & h_{12}^1 & \dots & h_{n-11}^1 & h_{n-12}^1 & h_{n1}^1 \\ -h_{02}^{1*} & h_{01}^{1*} & h_{12}^{1*} & -h_{11}^{1*} & \dots & (-1)^n h_{n-12}^{1*} & (-1)^{n-1} h_{n-11}^{1*} & (-1)^{n+1} h_{n2}^{1*} \\ h_{01}^3 & h_{02}^3 & h_{11}^3 & h_{12}^3 & \dots & h_{n-11}^3 & h_{n-12}^3 & h_{n1}^3 \\ \vdots & \vdots & \vdots & \vdots & \vdots & \vdots & \vdots & \vdots \\ -h_{02}^{2n-1*} & h_{01}^{2n-1*} & h_{12}^{2n-1*} & -h_{11}^{2n-1*} & \dots & (-1)^n h_{n-12}^{2n-1*} & (-1)^{n-1} h_{n-11}^{2n-1*} & (-1)^{n+1} h_{n2}^{2n-1*} \end{vmatrix},$$

$$\widetilde{(T_{rn})_{12}} = \begin{vmatrix} 0 & 1 & 0 & \lambda & \dots & 0 & \lambda^{n-1} & 0 \\ h_{01}^1 & h_{02}^1 & h_{11}^1 & h_{12}^1 & \dots & h_{n-11}^1 & h_{n-12}^1 & h_{n1}^1 \\ -h_{02}^{1*} & h_{01}^{1*} & h_{12}^{1*} & -h_{11}^{1*} & \dots & (-1)^n h_{n-12}^{1*} & (-1)^{n-1} h_{n-11}^{1*} & (-1)^{n+1} h_{n2}^{1*} \\ h_{01}^3 & h_{02}^3 & h_{11}^3 & h_{12}^3 & \dots & h_{n-11}^3 & h_{n-12}^3 & h_{n1}^3 \\ \vdots & \vdots & \vdots & \vdots & \vdots & \vdots & \vdots & \vdots \\ -h_{02}^{2n-1*} & h_{01}^{2n-1*} & h_{12}^{2n-1*} & -h_{11}^{2n-1*} & \dots & (-1)^n h_{n-12}^{2n-1*} & (-1)^{n-1} h_{n-11}^{2n-1*} & (-1)^{n+1} h_{n2}^{2n-1*} \end{vmatrix},$$

$$\widetilde{(T_{rn})_{21}} = \begin{vmatrix} 1 & 0 & \lambda & 0 & \dots & \lambda^{n-1} & 0 & 0 \\ h_{01}^1 & h_{02}^1 & h_{11}^1 & h_{12}^1 & \dots & h_{n-11}^1 & h_{n-12}^1 & h_{n2}^1 \\ -h_{02}^{1*} & h_{01}^{1*} & h_{12}^{1*} & -h_{11}^{1*} & \dots & (-1)^n h_{n-12}^{1*} & (-1)^{n-1} h_{n-11}^{1*} & (-1)^n h_{n1}^{1*} \\ h_{01}^3 & h_{02}^3 & h_{11}^3 & h_{12}^3 & \dots & h_{n-11}^3 & h_{n-12}^3 & h_{n2}^3 \\ \vdots & \vdots & \vdots & \vdots & \vdots & \vdots & \vdots & \vdots \\ -h_{02}^{2n-1*} & h_{01}^{2n-1*} & h_{12}^{2n-1*} & -h_{11}^{2n-1*} & \dots & (-1)^n h_{n-12}^{2n-1*} & (-1)^{n-1} h_{n-11}^{2n-1*} & (-1)^n h_{n1}^{2n-1*} \end{vmatrix},$$

$$\widetilde{(T_{rn})_{22}} = \begin{vmatrix} 0 & 1 & 0 & \lambda & \dots & 0 & \lambda^{n-1} & \lambda^n \\ h_{01}^1 & h_{02}^1 & h_{11}^1 & h_{12}^1 & \dots & h_{n-11}^1 & h_{n-12}^1 & h_{n2}^1 \\ -h_{02}^{1*} & h_{01}^{1*} & h_{12}^{1*} & -h_{11}^{1*} & \dots & (-1)^n h_{n-12}^{1*} & (-1)^{n-1} h_{n-11}^{1*} & (-1)^n h_{n1}^{1*} \\ h_{01}^3 & h_{02}^3 & h_{11}^3 & h_{12}^3 & \dots & h_{n-11}^3 & h_{n-12}^3 & h_{n2}^3 \\ \vdots & \vdots & \vdots & \vdots & \vdots & \vdots & \vdots & \vdots \\ -h_{02}^{2n-1*} & h_{01}^{2n-1*} & h_{12}^{2n-1*} & -h_{11}^{2n-1*} & \dots & (-1)^n h_{n-12}^{2n-1*} & (-1)^{n-1} h_{n-11}^{2n-1*} & (-1)^n h_{n1}^{2n-1*} \end{vmatrix},$$

$$\begin{aligned}
\widetilde{(Q_{rn})_{11}} &= \begin{vmatrix} h_{01}^1 & h_{02}^1 & h_{11}^1 & h_{12}^1 & \dots & h_{n-12}^1 & h_{n1}^1 \\ -h_{02}^{1*} & h_{01}^{1*} & h_{12}^{1*} & -h_{11}^{1*} & \dots & (-1)^{n-1}h_{n-11}^{1*} & (-1)^{n+1}h_{n2}^{1*} \\ h_{01}^3 & h_{02}^3 & h_{11}^3 & h_{12}^3 & \dots & h_{n-12}^3 & h_{n1}^3 \\ \vdots & \vdots & \vdots & \vdots & \vdots & \vdots & \vdots \\ -h_{02}^{2n-1*} & h_{01}^{2n-1*} & h_{12}^{2n-1*} & -h_{11}^{2n-1*} & \dots & (-1)^{n-1}h_{n-11}^{2n-1*} & (-1)^{n+1}h_{n2}^{2n-1*} \end{vmatrix}, \\
\widetilde{(Q_{rn})_{12}} &= - \begin{vmatrix} h_{01}^1 & h_{02}^1 & h_{11}^1 & h_{12}^1 & \dots & h_{n-11}^1 & h_{n1}^1 \\ -h_{02}^{1*} & h_{01}^{1*} & h_{12}^{1*} & -h_{11}^{1*} & \dots & (-1)^n h_{n-12}^{1*} & (-1)^{n+1}h_{n2}^{1*} \\ h_{01}^3 & h_{02}^3 & h_{11}^3 & h_{12}^3 & \dots & h_{n-11}^3 & h_{n1}^3 \\ \vdots & \vdots & \vdots & \vdots & \vdots & \vdots & \vdots \\ -h_{02}^{2n-1*} & h_{01}^{2n-1*} & h_{12}^{2n-1*} & -h_{11}^{2n-1*} & \dots & (-1)^n h_{n-12}^{2n-1*} & (-1)^{n+1}h_{n2}^{2n-1*} \end{vmatrix}, \\
\widetilde{(Q_{rn})_{21}} &= \begin{vmatrix} h_{01}^1 & h_{02}^1 & h_{11}^1 & h_{12}^1 & \dots & h_{n-12}^1 & h_{n2}^1 \\ -h_{02}^{1*} & h_{01}^{1*} & h_{12}^{1*} & -h_{11}^{1*} & \dots & (-1)^{n-1}h_{n-11}^{1*} & (-1)^n h_{n1}^{1*} \\ h_{01}^3 & h_{02}^3 & h_{11}^3 & h_{12}^3 & \dots & h_{n-12}^3 & h_{n2}^3 \\ \vdots & \vdots & \vdots & \vdots & \vdots & \vdots & \vdots \\ -h_{02}^{2n-1*} & h_{01}^{2n-1*} & h_{12}^{2n-1*} & -h_{11}^{2n-1*} & \dots & (-1)^{n-1}h_{n-11}^{2n-1*} & (-1)^n h_{n1}^{2n-1*} \end{vmatrix}, \\
\widetilde{(Q_{rn})_{22}} &= - \begin{vmatrix} h_{01}^1 & h_{02}^1 & h_{11}^1 & h_{12}^1 & \dots & h_{n-11}^1 & h_{n2}^1 \\ -h_{02}^{1*} & h_{01}^{1*} & h_{12}^{1*} & -h_{11}^{1*} & \dots & (-1)^n h_{n-12}^{1*} & (-1)^{n+1}h_{n1}^{1*} \\ h_{01}^3 & h_{02}^3 & h_{11}^3 & h_{12}^3 & \dots & h_{n-11}^3 & h_{n2}^3 \\ \vdots & \vdots & \vdots & \vdots & \vdots & \vdots & \vdots \\ -h_{02}^{2n-1*} & h_{01}^{2n-1*} & h_{12}^{2n-1*} & -h_{11}^{2n-1*} & \dots & (-1)^n h_{n-12}^{2n-1*} & (-1)^{n+1}h_{n1}^{2n-1*} \end{vmatrix}.
\end{aligned}$$

Here

$$h_{m,j}^l = \frac{\partial^l}{\partial \delta^l} ((d + i\frac{b}{2} + \delta^2)^m f_{1j}(\lambda_1 = d + i\frac{b}{2} + \delta^2))|_{\delta=0}, m = 0, 1, 2, \dots, n, j = 1, 2, l = 1, 2, \dots, 2n.$$

### References

- 
- [1] A.Hasegawa and F.Tappert, Appl.Phys.Lett. 23, 142-144 (1973).
- [2] S.L.McCall and E.L.Hahn, Phys.Rev.Lett. 18, 908-911 (1967).
- [3] A. I. Maimistov A I and E. A. Manykin, Sov. Phys.JETP 58, 685 (1983).
- [4] A.I. Maimistov and E. A. Manykin, Sov. Phys. JETP. 85, 1177-1181 (1983).
- [5] A. I. Maimistov and A. M. Basharov, Nonlinear Optical Waves (Springer-Verlag, Berlin, 1999).
- [6] K. Porsezian and K. Nakkeeran, J. Mod. Opt. 42,1953-1958 (1995).
- [7] S. Kakei and J. Satsuma, J. Phys. Soc. Japan 63, 885-894 (1994).
- [8] M. Nakazawa, E. Yamada and H. Kubota, Phys. Rev. Lett. 66,2625-2628(1991).
- [9] M. Nakazawa, E. Yamada and H. Kubota, Phys. Rev. A.44, 5973-5987 (1991).
- [10] M.Nakazawa, Y. Kimura, K. Kurokawa and K.Suzuki , Phys. Rev. A, 45, R23 (1992).
- [11] M.Nakazawa, K. Suzuki,Y. Kimura and H. Kubota , Phys. Rev. A 45 R2682 (1992).
- [12] K. Porsezian and K.Nakkeeran, Phys. Rev. Lett. 74, 2941-2944 (1995).
- [13] K. Porsezian, P. Seenuvasakumaran, and R. Ganapathy, Phys. Lett. A. 348, 233-243 (2006).
- [14] A.Mahalingam, K.Porsezian, M.S.Mani Rajan, and A.Uthayakumar, J. Phys. A: Math. Theor. 42, 165101 (2009).
- [15] C. G. Latchio Tiofack, Alidou. Mohamadou, Timoleon C Kofane and K. Porsezian, J. Opt. 12, 085202 (2010).
- [16] J.S.He, Y.Cheng and Y.S.Li, Commun. Theor. Phys.38, 493-496 (2002).
- [17] G.Neugebauer and R.Meinel, 1984, Phys.Lett.A. 100, 467-470 (1984).
- [18] V. B. Matveev and M.A. Salle, Darboux Transformations and Solitons (Springer-Verlag, Berlin, 1991).
- [19] Rui.G, Bo.T, Xing.L, Hai-Qiang.Zhang and Wen-

- Jun.Liu, Computational Mathematics and Mathematical Physics, 52, 565-577 (2012).
- [20] Ming Wang, Wen-Rui Shan, Xing L, Bo Qin, and Li-Cai Liu, Z.Naturforsch. 66a, 712-720 (2011).
- [21] C.Kharif and E.Pelinovsky, Eur.J.Mech.B (Fluids). 22, 603-634 (2003).
- [22] C.Kharif, E.Pelinovsky and A.Slunyaev, 2009, Rogue Waves in the Ocean (Berlin: Springer).
- [23] A.Chabchoub, N.P.Hoffmann and N.Akhmediev, Phys. Rev. Lett. 106,204502 (2011).
- [24] I.Didenkulova1 and E.Pelinovsky, Nonlinearity. 24, R1-R18 (2011).
- [25] D. H. Peregrine, J. Aust. Math. Soc. Ser. B, Appl. Math. 25, 16-43 (1983).
- [26] Kristian, B.Dysthe and K.Trulsen, Phys Scri. 82, 48-52 (1999).
- [27] V.E.Zakharov and L.A.Ostrovsky, Phys.D. 238, 540 (2009).
- [28] N.N.Akhmediev and V.I.Korneev, Theor. Math. Phys. 69, 1080-1093 (1986).
- [29] I.Shrira and V.Geogjaev, J.Eng.Math. 67, 11-22 (2010).
- [30] Zhenya.Yan, Phys. Lett.A. 374, 672-679 (2009).
- [31] ChaoQing Dai, GuoQuan Zhou and JieFang Zhang, Phys. Rev. E. 85, 016603(2012).
- [32] L.H.Ying,Z.Zhuang,E. J.Heller and L.Kaplan, Nonlinearity. 24, R67-R87 (2011).
- [33] P. Dubard, P. Gaillard, C. Klein, V.B. Matveev, Eur. Phys. J. Special Topics 185, 247-258 (2010).
- [34] P. Dubard, V.B. Matveev, Nat. Hazards. Earth. Syst. Sci. 11, 667-672 (2011).
- [35] P. Gaillard, J. Phys. A: Math.Theor. 44, 435204 (2011).
- [36] Boling.Guo,Liming.Ling and Q.P.Liu, Phys. Rev. E. 85, 026607(2012).
- [37] Yasuhiro. Ohta, Jianke. Yang, Proc. Proc.R. Soc.A 468, 1716 (2012).
- [38] N. Akhmediev, J. M. Soto-Crespo and A. Ankiewicz, Phys. Rev. A. 80, 043818 (2009).
- [39] J. S. He, H. R. Zhang, L. H. Wang, K. Porsezian and A. S. Fokas, 2012, A generating mechanism for higher order rogue waves, arXiv:1209.3742v3.
- [40] V. Fedun, M.S.Ruderman and R. Erdélyi, Phys. Lett.A. 372, 6107-6110 (2008).
- [41] M.S. Ruderman, Eur. Phys. Jour, 185, 57-66 (2010).
- [42] Shuwei. Xu, Jingsong.He and Lihong.Wang, J. Phys. A: Math. Theor.44, 305203 (2011).
- [43] Shuwei. Xu, Jingsong.He and Lihong.Wang, Europhys. Letter.97, 30007 (2012).
- [44] W.M.Moslem, P.K.Shukla and B.Eliasson, Euro.Phys.Lett. 96, 25002 (2011).
- [45] Boling Guo, Liming Ling and Q. P. Liu, Stud. Appl. Math. (2012) DOI: 10.1111/j.1467-9590.2012.00568.x.
- [46] D. R. Solli, C. Ropers, P. Koonath, and B. Jalali, Nature, 450, 1054-1057 (2007).
- [47] B. Kibler, J. Fatome, C. Finot, G. Millot, F. Dias, G. Genty, N. Akhmediev and J. M. Dudley, Nature. Physics. 6, 790-795 (2010).
- [48] F. T. Arecchi, U. Bortolozzo, A. Montina and S. Residori, Phys. Rev. Lett. 106, 153901 (2011).
- [49] A. Ankiewicz, J. M. Soto-Crespo and N. Akhmediev, Phys. Rev. E. 81, 046602 (2010).
- [50] Guangye Yang, Lu Li and Suotang Jia, Phys. Rev. E. 85, 046608(2012).
- [51] Yongsheng Tao and Jingsong He, Phys. Rev. E 85, 026601 (2012).
- [52] A. Ankiewicz, N. Akhmediev and J. M. Soto-Crespo, Phys. Rev. E. 82, 026602 (2010).
- [53] Boling.Guo and Liming.Ling, Chin. Phys. Lett. 28, 110202 (2011).
- [54] Fabio Baronio, Antonio Degasperis, Matteo Conforti and Stefan Wabnitz, 2012, Phys. Rev. Lett. 109, 044102(2012).
- [55] BaoGuo.Zhai, WeiGuo. Zhang, XiaoLiWang and HaiQiang Zhang, Nonlinear Anal. RWA 14, 14-27 (2012).
- [56] Zhenyun Qin and Gui Mu, Phys. Rev. E. 86, 036601(2012).
- [57] Rider. Jaimes-Reátegui, Ricardo. Sevilla-Escoboza and G.Huerta-Cuellar, Phys.Rev. Lett. 107, 274101 (2011).
- [58] V.E.Zakharov and A.B.Shabat, Soviet.Phys.JETP.37, 823-828(1973).
- [59] Jingsong. He, Shuwei. Xu and K. Porsezian, J. Phys. Soc. Jpn. 81, 033002 (2012).
- [60] J.S.He, L.Zhang, Y.Cheng and Y.S.Li, Science in China Series A: Mathematics.12, 1867-1878 (2006).
- [61] A. Ankiewicz, J.D. Kedziora, N. Akhmediev, Phys. Lett.A. 375, 2782-2785 (2011).
- [62] David.J. Kedziora, Adrian. Ankiewicz, and Nail. Akhmediev, Phys. Rev. E. 84, 056611 (2011).
- [63] J.M.Dudley and J.R.Taylor (Eds.), Supercontinuum Generation in Optical fibres(Cambridge,Cambridge University Press, 2010).
- [64] B.Kalithasan, K.Porsezian, P.T.Dinda and B.A.Malomed, J. Optics A: Pure and Applied Optics 11, 045205 (2009).
- [65] K.Porsezian,A.Hasegawa, V.N.Serkin, T.L. Belyaeva and R.Ganapathy, Phys. Lett. A., 361, 504-508 (2007).
- [66] V. N. Serkin and A. Hasegawa, Phys. Rev. Lett. 85, 4502 (2000).
- [67] V. N. Serkin, A. Hasegawa, and T. L. Belyaeva, Phys. Rev. Lett. 98, 074102 (2007).
- [68] V.N. Serkin, A. Hasegawa, T.L. Belyaeva, Journal of Modern Optics 57 , 1456 (2010).
- [69] Chuazhong Li, Jingsong He and K. Porsezian, arXiv:1205.1191v1 (2012).
- [70] Chuazhong Li and Jingsong He, arXiv:1210.2501 (2012).
- [71] Yu-Shan Xue, Bo Tian, Wen-Bao Ai, Min Li and Pan Wang Optics & Laser Technology, 48, 153-159(2013).

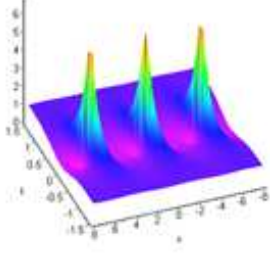


Fig. 1: The first order breather  $|E^{[1]}|^2$  given with specific parameters  $d = 1, b = 2, \omega_0 = \frac{1}{2}, \alpha_1 = \frac{4}{5}$ . There are one upper peak and two caves in each periodic unit.

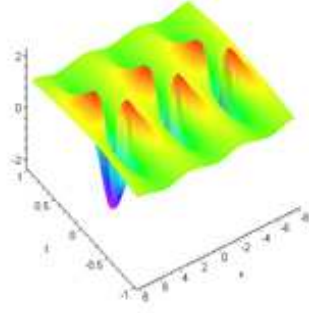


Fig. 3: The first order dark breather  $\eta^{[1]}$  for the values used in Figure 1. There are two lumps and one down peak in each periodic unit.

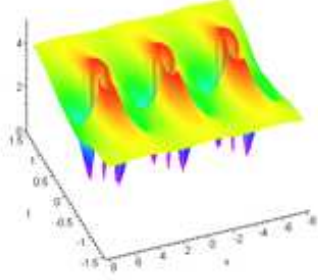


Fig. 2: The first order dark breather  $|p^{[1]}|^2$  for the values used in Figure 1. There are a upper ring and three down peaks in each periodic unit.

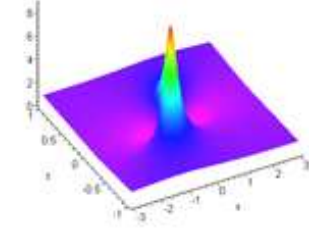


Fig. 4: The first order rogue wave  $|\tilde{E}^{[1]}|^2$  with specific parameters  $d = 1, b = 2, \omega_0 = \frac{1}{2}$ . There are one upper peak and two caves.

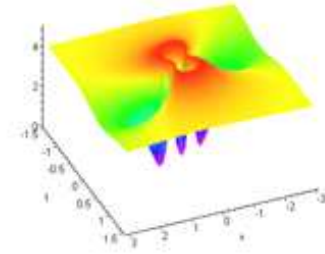


Fig. 5: The first order dark rogue wave  $|\tilde{p}^{[1]}|^2$  for the values used in Figure 4. There are one upper ring and three down peaks.

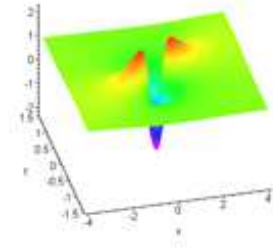


Fig. 6: The first order dark rogue wave  $\tilde{\eta}^{[1]}$  for the values used in Figure 4. There are two lumps and one down peak.



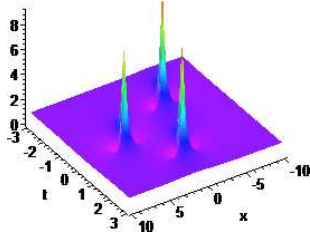


Fig. 7: The second order rogue wave  $|\bar{E}^{[2]}|^2$  given by eq.(25) with specific parameters  $d = 1, b = 2, \omega_0 = \frac{1}{2}, K_0 = 1, J_0 = 0, J_1 = 100$ .

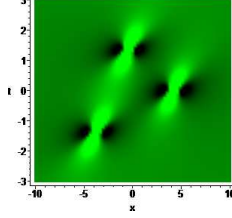


Fig. 8: Contour plot of the wave amplitudes of  $|\bar{E}^{[2]}|^2$  for the values used in Figure 7.

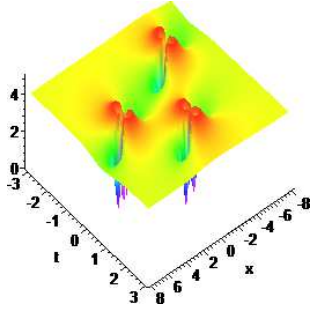


Fig. 9: The second order dark rogue wave  $|\bar{p}^{[2]}|^2$  given by eq.(26) for the values used in Figure 7.

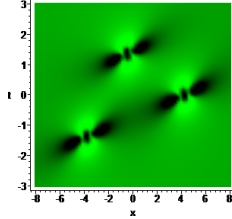


Fig. 10: Contour plot of the wave amplitudes of  $|\bar{p}^{[2]}|^2$  for the values used in Figure 7.

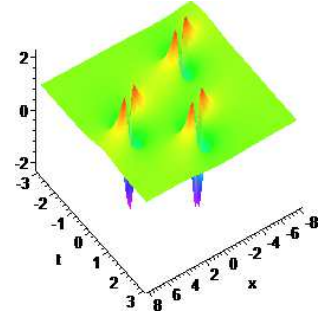


Fig. 11: The second order dark rogue wave  $\bar{\eta}^{[2]}$  given by eq.(27) for the values used in Figure 7.

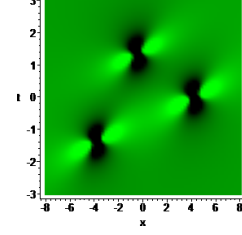


Fig. 12: Contour plot of the wave amplitudes of  $\bar{\eta}^{[2]}$  for the values used in Figure 7.

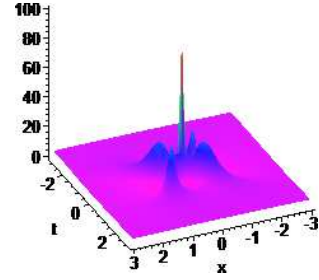


Fig. 13: The second order rogue wave  $|\bar{E}^{[2]}|^2$  given by eq.(25) with specific parameters  $d = 2, b = 0, \omega_0 = \frac{1}{2}, K_0 = 1, J_0 = 0, J_1 = 0$ .

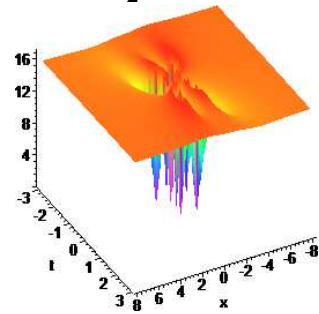


Fig. 14: The second order dark rogue wave  $|\bar{p}^{[2]}|^2$  given by eq.(26) for the values used in Figure 13.

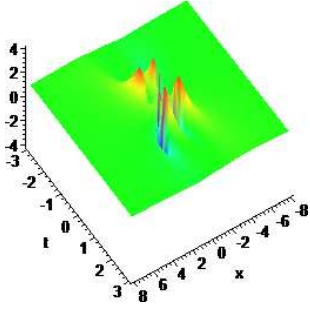


Fig. 15: The second order dark rogue wave  $\bar{\eta}^{[2]}$  given by eq.(27) for the values used in Figure 13.

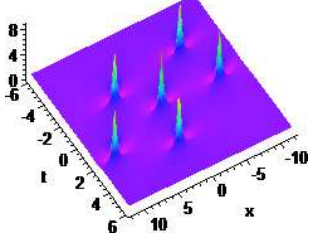


Fig. 16: The third order rogue wave  $|\bar{E}^{[3]}|^2$  given by eq.(25) with specific parameters  $d = 1, b = 2, \omega_0 = \frac{1}{2}, K_0 = 1, J_0 = 0, J_1 = 0, J_2 = 8000$ .

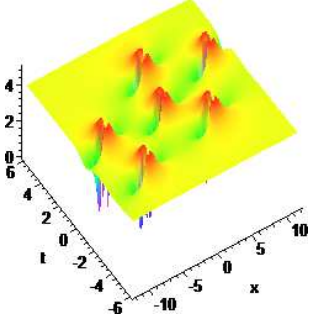


Fig. 17: The third order dark rogue wave  $|\bar{p}^{[3]}|^2$  given by eq.(26) for the values used in Figure 16.

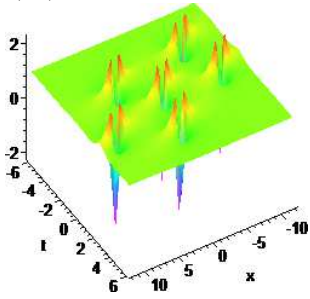


Fig. 18: The third order dark rogue wave  $\bar{\eta}^{[3]}$  given by eq.(27) for the values used in Figure 16.

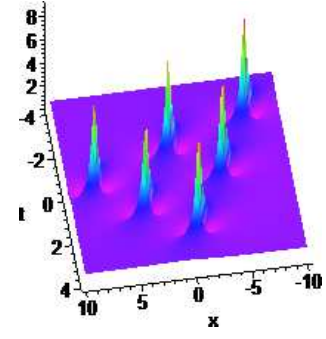


Fig. 19: The third order rogue wave  $|\bar{E}^{[3]}|^2$  given by eq.(25) with specific parameters  $d = 1, b = 2, \omega_0 = \frac{1}{2}, K_0 = 1, J_0 = 0, J_1 = 100, J_2 = 0$ .

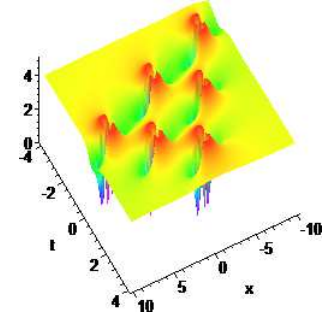


Fig. 20: The third order dark rogue wave  $|\bar{p}^{[3]}|^2$  given by eq.(26) for the values used in Figure 19.

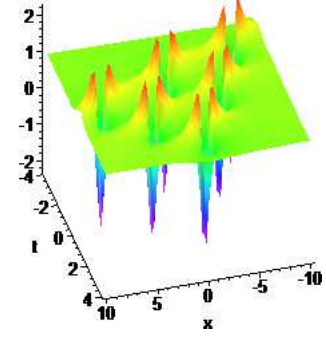


Fig. 21: The third order dark rogue wave  $\bar{\eta}^{[3]}$  given by eq.(27) for the values used in Figure 19.

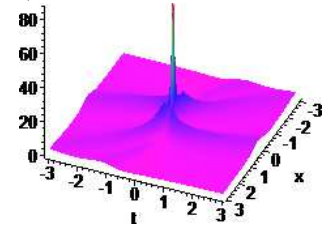


Fig. 22: The third order rogue wave  $|\bar{E}^{[3]}|^2$  given by eq.(25) with specific parameters  $d = \frac{4}{3}, b = 0, \omega_0 = \frac{1}{2}, K_0 = 1, J_0 = 0, J_1 = 0, J_2 = 0$ .

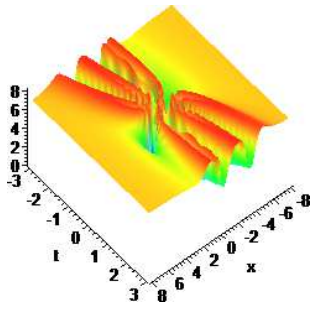


Fig. 23: The third order dark rogue wave  $|\bar{p}^{[3]}|^2$  given by eq.(26) for the values used in Figure 22.

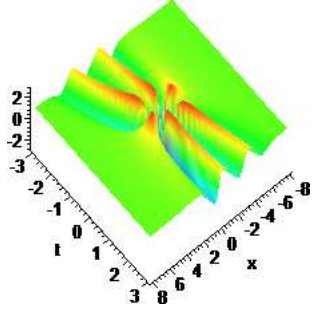


Fig. 24: The third order dark rogue wave  $\bar{\eta}^{[3]}$  given by eq.(27) for the values used in Figure 22.